Juanes-Garcia et al., http://www.jcb.org/cgi/content/full/jcb.201407059/DC1

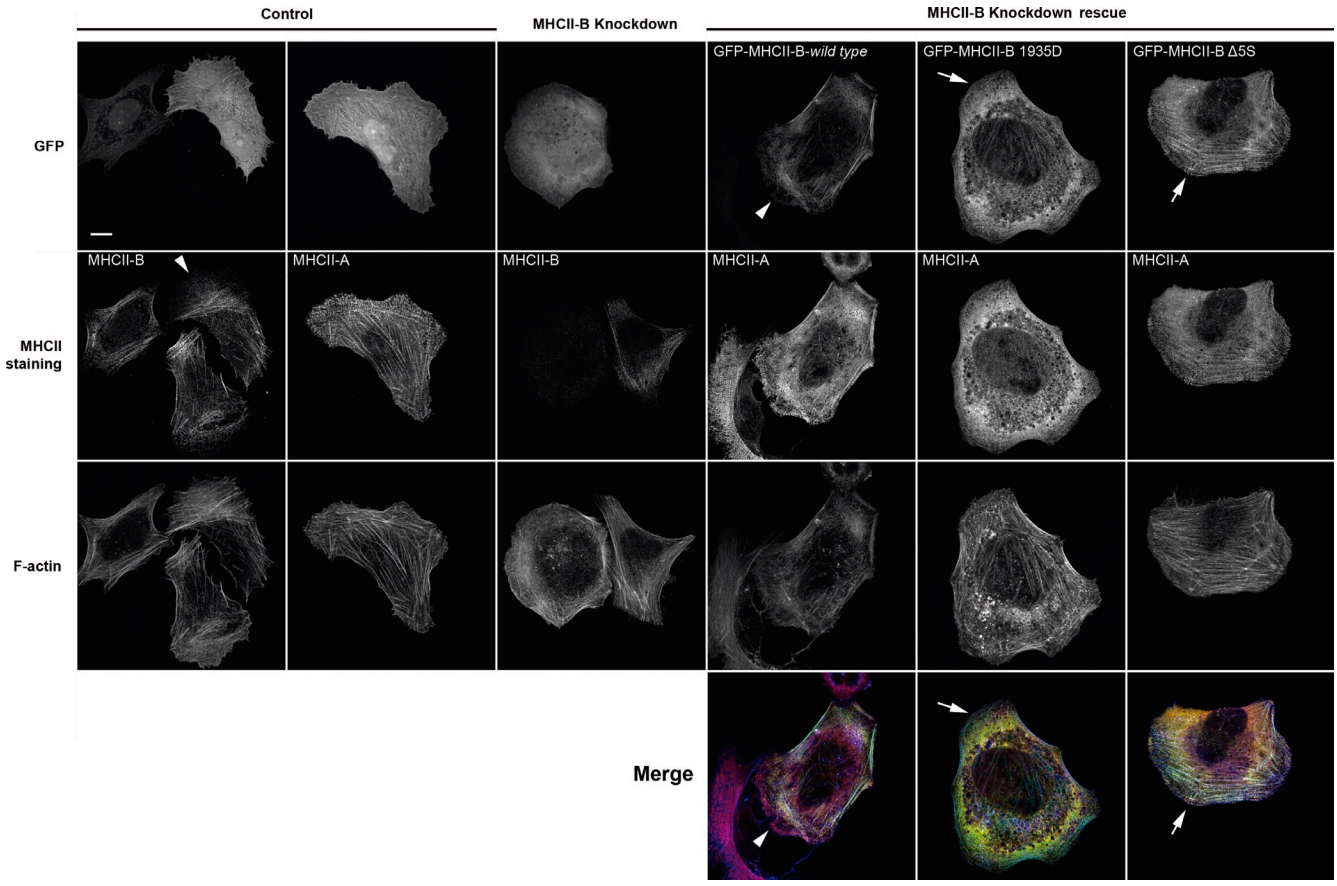

Figure S1. **Effect of MHCII-B depletion and rescue with MHCII-B mutants in U-2 OS cells.** Control U2OS transfected with GFP and scrambled pSUPER (first two columns), depleted of endogenous MHCII-B using pSUPER–MHCII-B (third column), or depleted of endogenous MHCII-B and rescued with GFP-coupled, wild-type MHCII-B (fourth column), MHCII-B 1935D (fifth column), or MHCII-B Δ5S (last column) were allowed to adhere to fibronectin for 2 h and stained for the indicated MHCII isoform (middle row) and F-actin (bottom row). Arrowheads point to protrusions with low concentration of NMII-B that display a gradient-wise increment of MHCII-B toward the center of the cell. Arrows point to protrusions prominently decorated with the indicated mutants and a barely detectable localization gradient. Bar, 10 µm.

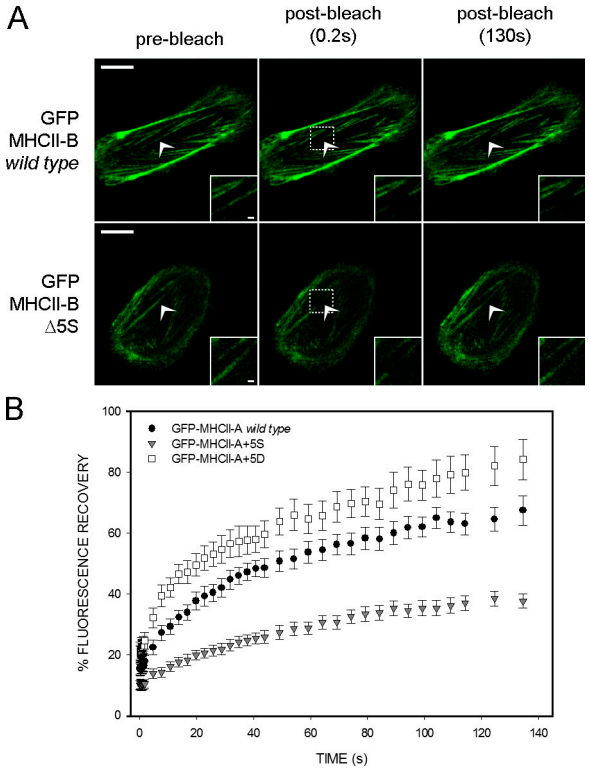

Figure S2. **Representative FRAP sequence.** (A) Snapshots of a confocal time-lapse video of CHO.K1 cells transfected with wild-type GFP–MHCII-B (top row) or GFP–MHCII-B Δ5S (bottom row). Arrowheads indicate the regions of interest that contain the bleached GFP-decorated myosin bundle. The first snapshot shows the cell before photobleaching (prebleach). The second snapshot corresponds to a time point captured immediately after photobleaching. The third snapshot represents one of the last scans after photobleaching. Insets are close-ups of the indicated areas (boxes). See Materials and methods for additional technical information. Bars: (main images) 10 µm; (insets) 1 µm. (B) Insertion of a negatively charged cluster adjacent to P1927 in MHCII-A does not increase its stability in actomyosin bundles. FRAP curve of GFP–MHCII-A+5D showing increased fractional recovery compared with GFP–MHCII-A wild type. The curve of GFP–MHCII-A+5S used in Fig. 1 G is shown again for reference. Data are the means ± SEM of 24 individual measurements per condition in four independent experiments.

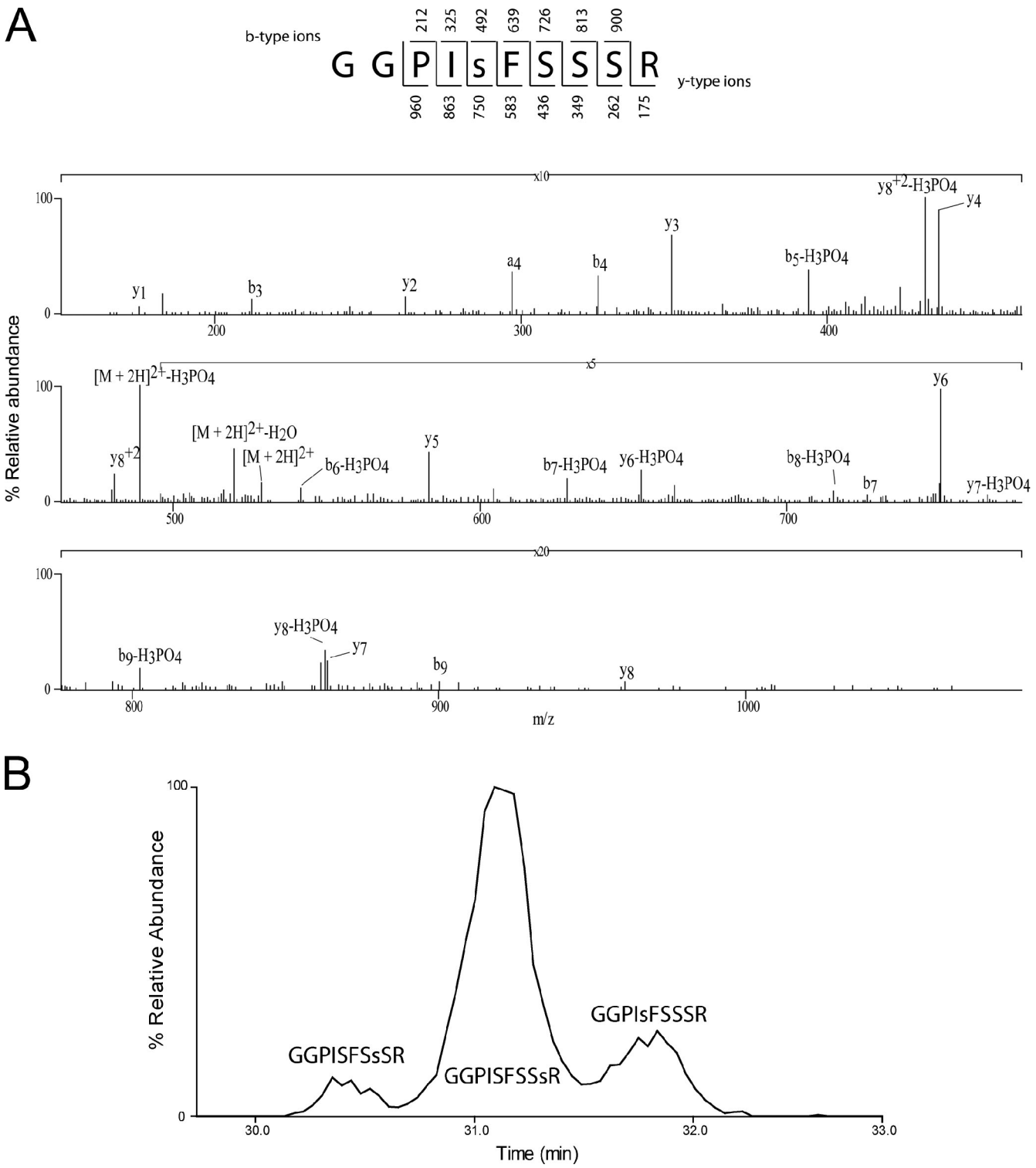

Figure S3. **MS/MS spectrum of phosphorylated Ser1935.** (A) CAD MS/MS spectrum acquired in the ion trap of an Front End Electron Transfer Dissociation enabled LTQ-FT of the $[M + 2H]^{2+}$ ion (mass per charge [m/z] of 537.73) corresponding to the endogenous MHCII-B tryptic peptide GGPIsFSSSR phosphorylated on Ser1935. Identified product ions of the b′ and y′ types are indicated in the spectrum and by underlining in the peptide sequence and are sufficient to determine that the spectrum is that of the peptide phosphorylated on Ser1935. (B) Extracted ion chromatogram of endogenous monophosphorylated MIIB peptide Gly1931–Arg1940 with the three different detected phosphorylations. Data are representative of three experiments performed.

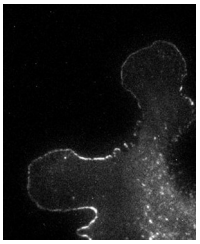

Video 1. **Loss of adhesion elongation in MHCII-A–depleted CHO.K1 cells.** MHCII-A–depleted CHO.K1 cells were cotransfected with paxillin-mCherry (single channel) and allowed to migrate on fibronectin. TIRF images were captured in a TIRF microscope (IX70; Olympus) coupled to a CCD camera (Retiga EXi; QImaging). Frames were taken every 5 s for 12.5 min.

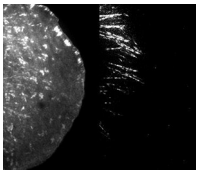

Video 2. **Restoration of adhesion elongation in MHCII-A-depleted CHO.K1 cells rescued with wild type GFP–MHCII-A.** MHCII-A–depleted CHO.K1 cells were cotransfected with paxillin-mCherry (left) and wild-type GFP–MHCII-A (right) and allowed to migrate on fibronectin. TIRF images were captured in a TIRF microscope (IX70; Olympus) coupled to a CCD camera (Retiga EXi; QImaging). Frames were taken every 5 s for 12.5 min.

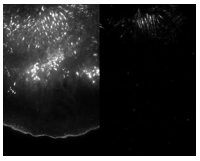

Video 3. **Lack of restoration of adhesion elongation in MHCII-A–depleted cells rescued with GFP–MHCII-A+5S, which is positioned away from the protrusion.** MHCII-A–depleted CHO.K1 cells were cotransfected with paxillin-mCherry (left) and GFP–MHCII-A+5S (right) and allowed to migrate on fibronectin. TIRF images were captured in a TIRF microscope (IX70; Olympus) coupled to a CCD camera (Retiga EXi; QImaging). Frames were taken every 5 s for 16.6 min.

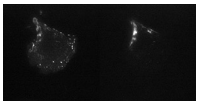

Video 4. **Stable front–rear polarization of MHCII-B–depleted CHO.K1 cells rescued with wild-type GFP–MHCII-B.** MHCII-B–depleted CHO.K1 cells were cotransfected with mCherry-vinculin (left) and wild-type GFP–MHCII-B (right) and allowed to migrate on fibronectin. TIRF images were captured in a TIRF microscope (IX83/TIRF Mitico; Olympus) coupled to an electron-multiplying CCD camera (ImagEM X2; Hamamatsu Photonics). Frames were taken every 30 s for 50 min.

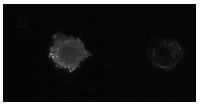

Video 5. **Loss of stable front–rear polarization in MHCII-B–depleted CHO.K1 cells rescued with GFP–MHCII-B 1935D.** MHCII-B–depleted CHO.K1 cells were cotransfected with mCherry-vinculin (left) and GFP-MHCII-B 1935D (right) and allowed to migrate on fibronectin. TIRF images were captured in a TIRF microscope (IX83/TIRF Mitico; Olympus) coupled to an electron-multiplying CCD camera (ImagEM X2; Hamamatsu Photonics). Frames were taken every 30 s for 50 min.

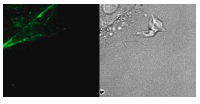

Video 6. **Localization of wild-type GFP–MHCII-B away from the protrusion in CHO.K1 cells rescued with wild-type GFP–MHCII-B.** MHCII-B–depleted CHO.K1 cells were transfected wild-type GFP–MHCII-B (green) and allowed to migrate on fibronectin. Phase-contrast images are shown on right. Confocal images were captured in a laser-scanning confocal microscope (SP5; Leica). Frames were taken every 9 s for 20 min.

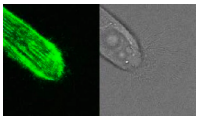

Video 7. **Anterior localization of GFP–MHCII-B 1935D in CHO.K1 cells rescued with GFP–MHCII-B 1935D.** MHCII-B–depleted CHO.K1 cells were transfected GFP–MHCII-B 1935D (green) and allowed to migrate on fibronectin. Phase-contrast images are shown on right. Confocal images were captured in a laser-scanning confocal microscope (SP5; Leica). Frames were taken every 9 s for 20 min.